

# On the UWB System Coexistence With GSM900, UMTS/WCDMA, and GPS

Matti Hämäläinen, *Student Member, IEEE*, Veikko Hovinen, *Student Member, IEEE*,  
Raffaello Tesi, *Student Member, IEEE*, Jari H. J. Iinatti, *Member, IEEE*, and Matti Latva-aho, *Member, IEEE*

**Abstract**—This paper evaluates the level of interference caused by different ultra-wideband (UWB) signals to other various radio systems, as well as the performance degradation of UWB systems in the presence of narrowband interference and pulsed jamming. The in-band interference caused by a selection of UWB signals is calculated at GSM900, UMTS/wideband code-division multiple-access (WCDMA), and global position system (GPS) frequency bands as a function of the UWB pulsewidth. Several short-pulse waveforms, based on the Gaussian pulse, can be used to generate UWB transmission. The two UWB system concepts studied here are time hopping and direct sequence spread spectrum. Baseband binary pulse amplitude modulation is used as the data modulation scheme. Proper selection of pulse waveform and pulsewidth allows one to avoid some rejected frequency bands up to a certain limit. However, the pulse shape is also intertwined with the data rate demands. If short-pulses are used in UWB communication the high-pass filtered waveforms are preferred according to the results. The use of long pulses, however, favors the generic Gaussian waveform instead. An UWB system suffers most from narrowband systems if the narrowband interference and the nominal center frequency of the UWB signal overlap. This is proved by bit-error rate simulations in an additive white Gaussian noise (AWGN) channel with interference at global system for mobile communication (GSM) and UMTS/WCDMA frequencies.

**Index Terms**—Bit-error rate (BER), coexistence, direct-sequence (DS), impulse radio (IR), interference, pulse amplitude modulation, time-hopping (TH), ultra-wideband (UWB).

## I. INTRODUCTION

ULTRA-WIDEBAND (UWB) technology is one of the possible solutions for future short-range indoor data communication applications. The Federal Communication Commission (FCC) defines a radio system to be an UWB system if the fractional bandwidth  $B_f$  or the  $-10$  dB bandwidth of the signal is greater than 20% or greater than 500 MHz, respectively [1]. UWB technology offers simultaneously high data rate communication and high accuracy positioning capabilities. These systems can utilize low transmitted signal power level with extremely wide bandwidth. Due to the noiselike signal characteristics the UWB systems can co-exist with the other radio systems. The UWB concept can be based on, for example,

time-hopping (TH), direct-sequence (DS) spread-spectrum approaches, fast frequency sweeping, or multicarrier techniques. In this paper, we study the UWB techniques based both on TH and DS. The data modulation schemes most often used in UWB systems are pulse position modulation (PPM) and pulse amplitude modulation (PAM). Probably the best known UWB system for data communication is so called impulse radio (IR) that utilizes TH-PPM [2].

Pulsed UWB signal is generated by using sub-nanosecond pulses that spread the signal energy over on extremely wide frequency band. One data bit is spread over multiple pulses, and a train of base-band pulses is sent through the radio channel. This spreading corresponds to pulse repetition coding, which gives processing gain, allowing low signal-to-noise ratios (SNRs) and avoiding interference or jamming at the receiver-end.

User separation in UWB systems can be done using independent pseudorandom (PR) codes for each user, similar to code-division multiple-access (CDMA) systems. Discontinuous transmission in TH UWB systems, also gives robustness against severe multipath propagation. As long as the pulse repetition interval is larger than the delay spread of the channel, interpulse interference can be avoided.

The preliminary approval of UWB technology made by FCC reserves the frequency band between 3.1 and 10.6 GHz for indoor UWB communication systems [1]. Since this work has been carried out before the FCC approval, the frequency bands for the studied UWB transmission go beyond the limits.

In this paper, we have studied the in-band interference power caused by different kinds of UWB signals at some predefined frequency bands. The interference levels are studied as functions of the UWB pulsewidth at the frequency bands of GSM900, UMTS/WCDMA, and GPS. The pulsewidth of an UWB system depends on the data rate and it is typically on the order of 1 ns or less. This study covers a selection of pulsewidths between 0.2 and 3.5 ns. Also, the UWB system performance degradation in additive white Gaussian noise (AWGN) channel in the presence of narrowband interference is studied. The interfering systems taken into account are GSM and UMTS/WCDMA.

The paper is organized as follows. First, Section II gives a short introduction to the UWB systems based on TH and DS concepts. Section III presents the numerical results for the in-band interference simulations in GSM, UMTS/WCDMA and GPS frequency bands. In Section IV, the effect of narrowband interference on the UWB system performance degradation are studied using GSM and UMTS/WCDMA systems as an interference source. Finally, the conclusions are given in Section V.

Manuscript received December 3, 2001; revised June 24, 2002. This paper was supported in part by The National Technology Agency of Finland (Tekes), Nokia, Elektrobot, and in part by the Finnish Defense Forces.

The authors are with the Centre for Wireless Communication, University of Oulu, FIN-90014 Oulu, Finland (e-mail: matti.hamalainen@ee.oulu.fi).

Digital Object Identifier 10.1109/JSAC.2002.805242

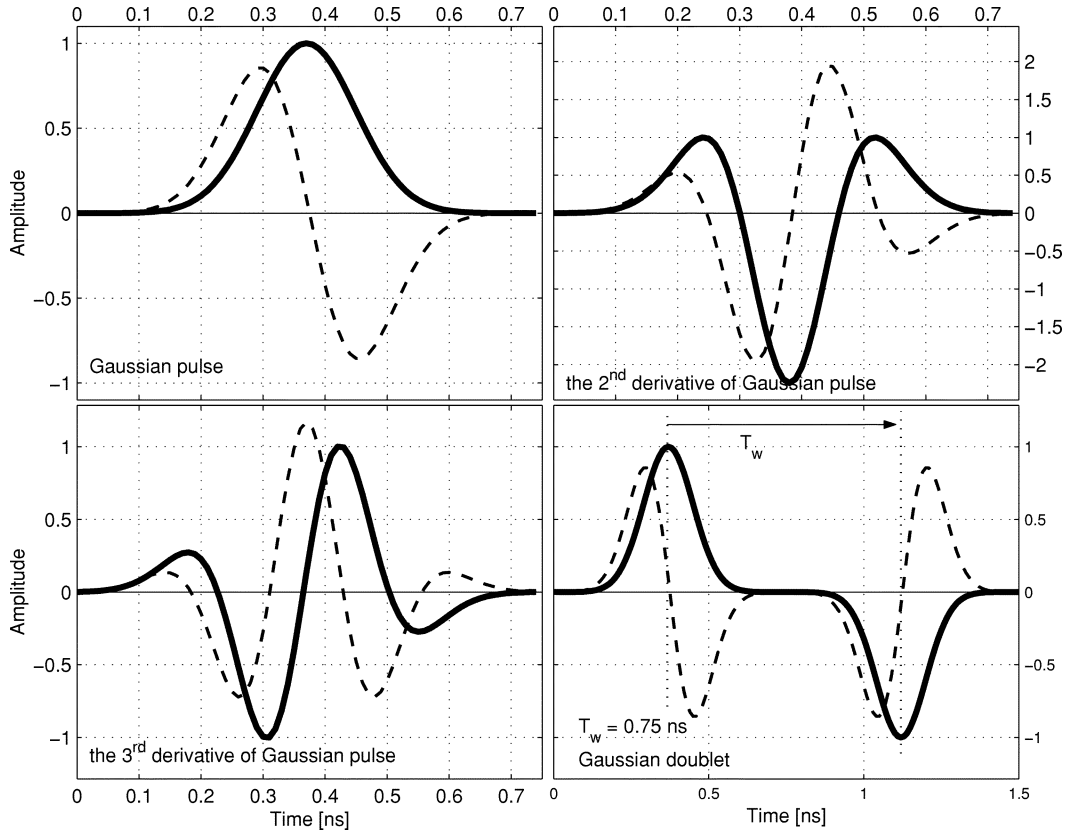


Fig. 1. Pulse waveforms used in the study; solid thick lines represent the generated pulses, dashed thin lines represent the pulse waveforms in the channel.

## II. UWB SYSTEM MODELS

### A. Pulse Waveforms

The spectral properties of an UWB signal depend on the pulse waveform, as well as on the pulsewidth. The use of very narrow pulses spreads the transmitted signal energy to an extremely wide frequency band. In this paper, we have selected several pulse waveforms, based on the generic Gaussian pulse, for detailed study. The simplest one is the Gaussian pulse itself [2]. Two amplitude reversed Gaussian pulses with time gap  $T_w$  between the pulses are used to form a bipolar signal called Gaussian doublet [3]. The other waveforms are high-pass filtered versions of the basic Gaussian pulse, simply modeled as higher derivatives of the generic pulse.

In time domain, the Gaussian pulse can be mathematically defined as

$$w(t) = \frac{1}{\sigma\sqrt{2\pi}} \exp\left(-0.5 \left(\frac{t-\mu}{\sigma}\right)^2\right) \quad (1)$$

where  $\sigma$  is the standard deviation and  $\mu$  is the mean value of the Gaussian distribution, respectively.

The effects of antennas can be modeled as a differentiation operation [4], [5]. Therefore, the pulse waveforms in the channel are the first derivatives of the generated pulses. If a loop antenna is used the pulse waveform in the channel is the second derivative of the generated pulse [5]. The receiving antenna differentiates the received pulse waveform correspondingly. The generated pulse waveforms and the corresponding waveforms

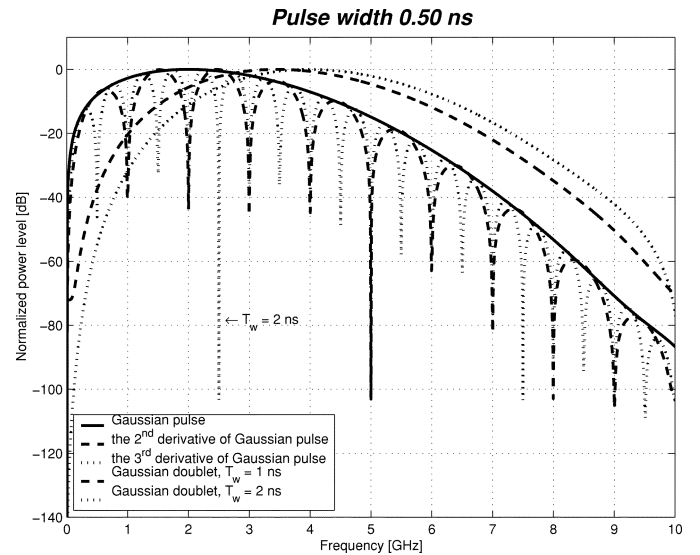


Fig. 2. Normalized power spectral densities for the different UWB pulses. In all cases, pulsewidth  $T_p = 0.5$  ns.

in the channel are presented in Fig. 1. Fig. 2 presents the corresponding spectra of the radiated pulses (in the example,  $T_p = 0.5$  ns).

As one can notice from Fig. 2, the generic Gaussian pulse and the Gaussian doublet have similar spectral envelopes. This is because they have the same basic pulse waveform. However, with the doublet, regular nulls in the frequency domain emerge. The null separation on the frequency axis is inversely proportional to the pulse separation  $T_w$  within the doublet. All pulse

TABLE I  
CENTER FREQUENCIES AND  $-10$ -dB BANDWIDTHS  
FOR THE USED PULSE WAVEFORMS

Generated pulse waveform	$f_c$	$B_{-10dB}$
A) Gaussian pulse	$1/T_p$	$2/T_p$
B) Gaussian doublet	$1/T_p$	$2/T_p$
C) the 2 <sup>nd</sup> derivative of A	$1.73/T_p$	$2.1/T_p$
D) the 3 <sup>rd</sup> derivative of A	$2/T_p$	$2/T_p$

waveforms used here have asymmetric spectra about the center frequency which is assumed to be the frequency having the maximum power level. Table I expresses the relationships between the pulsewidth, the center frequency and the  $-10$  dB bandwidth for the used pulse waveforms.

### B. System Concepts

The two UWB systems studied here are based on TH-UWB and on DS-UWB concepts. In both cases, one transmitted data bit is spread over multiple pulses to achieve a processing gain in reception due to repetition code.

The binary baseband pulse amplitude modulated (BPAM) information signal  $s(t)$  for the  $m$ th user can be presented as

$$s^{(m)}(t) = \sum_{k=-\infty}^{\infty} \sum_{j=1}^N w(t - kT_d - jT_f - (c_w)_j^{(m)}T_c) d_k^{(m)} \quad (2)$$

for TH and

$$s^{(m)}(t) = \sum_{k=-\infty}^{\infty} \sum_{j=1}^N w(t - kT_d - jT_c)(c_p)_j^{(m)} d_k^{(m)} \quad (3)$$

for DS, where  $d_k$  is the  $k$ th data bit,  $(c_p)_j$  is the  $j$ th chip of the PR code,  $(c_w)_j$  is the  $j$ th code phase defined by the PR code, and  $w(t)$  is the pulse waveform.  $N$  represents the number of pulses to be used per databit,  $T_c$  is the chip length, and  $T_f$  is the nominal pulse repetition interval. Both the PR code and the data are bipolar, thus having values  $\{-1, +1\}$ . Bit length is  $T_d = NT_c$  in DS-UWB and  $T_d = NT_f$  in TH-UWB. Furthermore, in DS-UWB, we have  $T_c = T_p = T_f$ . The ideas of TH-UWB and DS-UWB concepts are presented in Fig. 3.

In TH-UWB systems, the PR code defines the transmission instants inside TH frames, for each user individually. In DS-UWB systems, one data bit is spread over multiple pulses using a PR code like in conventional DS spread spectrum concepts. The chip waveforms are shown in Fig. 1. The pulse repetition interval (frame length)  $T_f$  in TH-UWB is much longer than the pulsewidth  $T_p$ . In this study, the PR code used is a bipolar maximum length code, unless otherwise stated. Because both of the UWB concepts use bipolar PR code and bipolar data, either the pulse, or its amplitude-reversed version, is transmitted to the channel.

A PR code is used to separate the users (CDMA) and to smooth the spectrum. If the pulse repetition interval in UWB system is fixed, line spectrum will arise. The separation between

the consecutive spectral lines is inversely proportional to the pulse repetition interval. These spectral lines need to be avoided, in order to reduce the interference caused to other radio systems.

The data rate  $R_d$  in UWB systems can be calculated as

$$R_d = 1/NT_f. \quad (4)$$

If the number of transmitted pulses per data bit and the pulsewidth are fixed to the same values in both concepts, the data rate in TH concept is smaller than in DS, because  $T_{f,TH-UWB} > T_{f,DS-UWB}$ . In DS-UWB, the pulse transmission is continuous, but in TH-UWB, there are silent periods between the consecutive pulses, as shown in Fig. 3.

If the aim is, in both TH-UWB and DS-UWB concepts, to keep the pulsewidth and the data rate fixed at the same value less pulses need to be sent in TH than in DS. This has an effect on the single pulse power levels. In TH-UWB systems, if the energy of the data bit is fixed, the energy of a single pulse should be increased to maintain the whole system performance at the same level. The processing gain in both systems still remains the same, due to the extra processing gain from the low duty cycle in the TH-concept.

In UWB systems, the pulsewidth and the pulse waveform define the spectrum of the transmitted signal and not the data rate. This allows one to select the optimal waveform giving minimum interference at certain rejected frequency bands. The data rate of the system depends on the spreading factor and the pulse repetition interval, as noted by (4). In DS-UWB systems, the pulsewidth is defined by the spreading factor (code length  $N$ ), if the whole code period is used to send one data bit.

### C. Simulation Assumptions

There are several approaches one can take when studying UWB system spectral coexistence. For example, the data rate of the studied system can be fixed. If the processing gain is kept the same, TH-UWB and DS-UWB have different pulsewidths. Thus, the systems are using different parts of the frequency spectrum. Moreover, the power of a single pulse in the TH system is higher than in the corresponding DS pulse.

In our approach, the bit energy and the spreading factor of the UWB concepts are fixed. The interference level is measured as a function of the pulsewidth from a "victim receiver" point of view and the UWB system performance is not considered in this context. This approach sets the spectra of the TH and DS systems to the same location in the frequency domain, and thus, the interference results are comparable.

The numerical results of the following sections represent worst case scenarios from the interference point of view. This is due to the fact that the effects of the radio channel (e.g., signal attenuation, multipath propagation) are not taken into account. Using these results, one can compare the relative ratio of the interference for different pulse waveforms, from the victim receiver's point of view. The plotted interfering powers can be interpreted as transmitted powers radiated straight after the transmitter antenna and measured using an ideal probe. The energy coupling from the transmitter antenna to the monitoring probe is assumed to be perfect, so that all the radiated energy will be detected. In real life, the interference is less, due to the signal attenuation in the radio channel and nonideal antenna coupling.

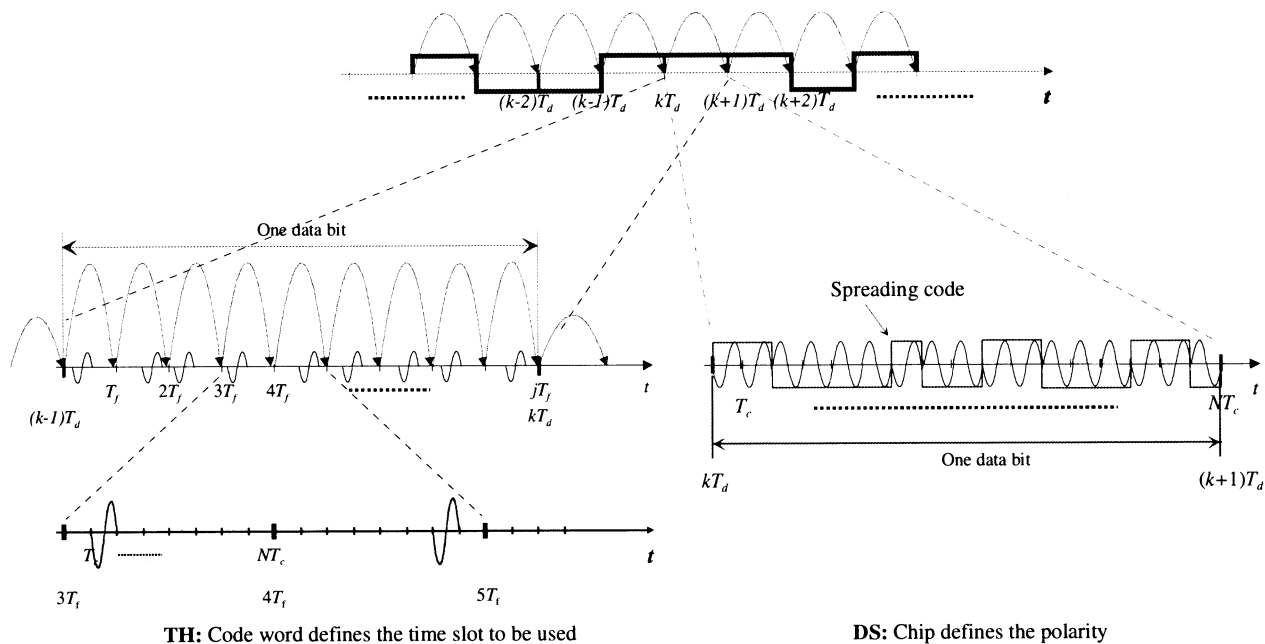


Fig. 3. Difference between the TH-UWB and DS-UWB concepts.

When composing the UWB signal, one data bit is spread over  $N$  pulses, and the pulse train is Fourier transformed to get the frequency-domain spectrum. The interfering power caused by an UWB signal  $P_I$  is calculated from the amplitude spectrum  $S(f)$  inside a victim receiver's bandwidth  $B$  using the formula

$$P_I = \sum_{i \in B} |S_i(f)|^2. \quad (5)$$

The frequency resolution of the amplitude spectrum  $\Delta f$  is defined by the sample interval  $\Delta t$ , and the number of points used in the fast Fourier transform (FFT)  $N_{\text{FFT}}$ , as given by

$$\Delta f = \frac{1}{\Delta t / N_{\text{FFT}}}. \quad (6)$$

The sample interval is defined by the frame structure, and the number of samples taken from the pulse waveform as preferred in the equation

$$\Delta t = \frac{T_f}{\lceil T_f N_{\text{sp}} / T_p \rceil} \quad (7)$$

where  $N_{\text{sp}}$  is the number of samples within the pulse, and  $\lceil \cdot \rceil$  takes the highest integer value that is smaller or equal than the operand. The number of taken FFT points in the Fourier transform can be defined using the equation

$$N_{\text{FFT}} = 2^{\left\lceil \frac{\log \frac{N_{\text{ss}}}{B \Delta t}}{\log 2} \right\rceil} + 1 \quad (8)$$

where  $N_{\text{ss}}$  gives the number of frequency samples taken within the victim receiver's frequency band  $B$ . The ratio between the calculated frequency samples and the FFT size needed is plotted in Fig. 4.

$N_{\text{FFT}}$  is the limiting parameter during the simulations. Increasing  $N_{\text{FFT}}$ , the computational demands are also increased. To achieve a high enough frequency resolution for reliable results, a large number of samples from the amplitude spectrum need to be taken. This enables a quite small spreading factor

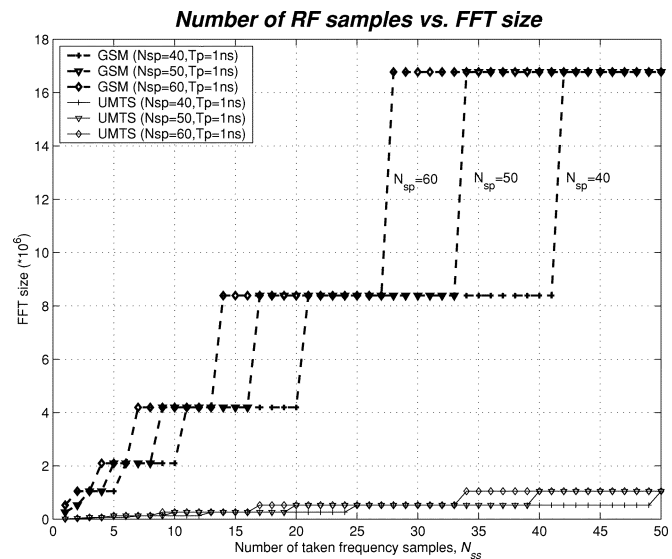


Fig. 4. Number of frequency samples and the corresponding FFT size.

to be used in the case of GSM. The smaller the frequency resolution, the more FFT points are needed. In fact, 200-kHz GSM channel bandwidth leads to the FFT size of over 8 million to achieve the high-frequency resolution for the defined pulse train, as presented in Fig. 4.

In all the cases studied, the total UWB power over one data bit is fixed to  $P_d = 0.5$  mW. The bit energy is evenly spread over the pulses corresponding to the databit. The temporary bandwidths of the interfering UWB signals both in TH-UWB and DS-UWB modes are equal because the corresponding  $T_p$ s remain the same. The pulse power needed to satisfy a certain bit power assumption is a function of the pulse spreading factor  $N$ . If  $N$  is increased the pulse power can be decreased for an individual pulse. This means that less interference is generated to the other radio systems frequencies.

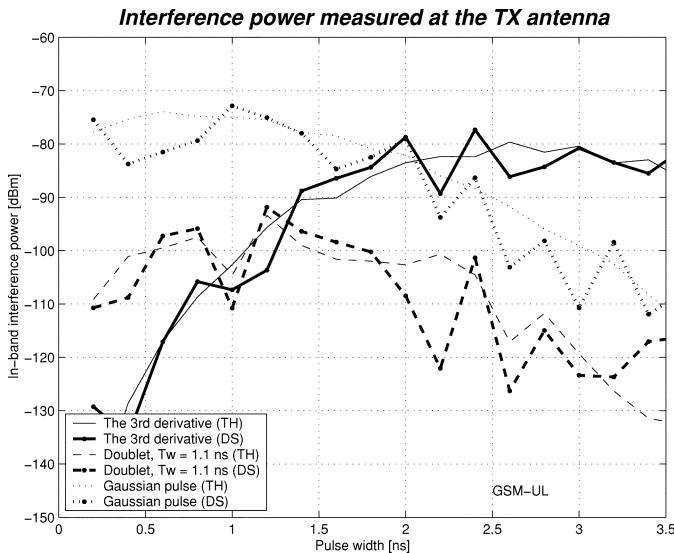


Fig. 5. In-band interference power as a function of the pulsewidth at GSM900 UL band.

### III. IN-BAND INTERFERENCE CAUSED BY UWB TRANSMISSION

This section introduces the in-band interference calculation results at the following victim receiver bands: GSM900, UMTS/WCDMA, and GPS. A random physical channel in the middle of a victim system bandwidth has been selected for the interference calculations. The in-band interference power is calculated over the victim receiver's bandwidth.

In the simulations, a train of pulses is generated using random databits and a fixed pulse spreading factor. The pulse train is Fourier transformed to get the amplitude spectrum of the signal. The interference is calculated using the samples of the amplitude spectra of the transmitted UWB signal, as noted in (5).

In this paper, the used pulsewidths cover the range from 0.2 to 3.5 ns (maximum). This corresponds to a center frequency range from 0.25 to 10 GHz depending on the pulse waveform used (see Table I). All system assumptions are fixed during the same victim system study, so that the results are comparable.

#### A. UWB Interference at the GSM900 Bands

In the following, the in-band interference is studied from a GSM900 system point of view. GSM system utilizes a frequency division duplex (FDD). The uplink (UL) and the downlink (DL) bands in Europe are 890 915 and 935 960 MHz, respectively, and the channel bandwidth (physical channel) is 200 kHz [6]. Both the UL and the DL bands have been considered. The interference powers are calculated in the middle of both of the bands, and the results can be expanded to cover also the rest of the corresponding bands.

Results covering the interference study in GSM uplink can also be found from [7]. Those results are discussed here in more detail. Also, the DL band, which was not included in [7], is also covered here.

The in-band interference power depends on the spectral allocation of the interfering UWB signal. This can be noticed from Figs. 5 and 6. When the pulsewidth changes, the spectral allocation of the corresponding waveform in the frequency domain also changes. For a certain pulsewidth, the UWB

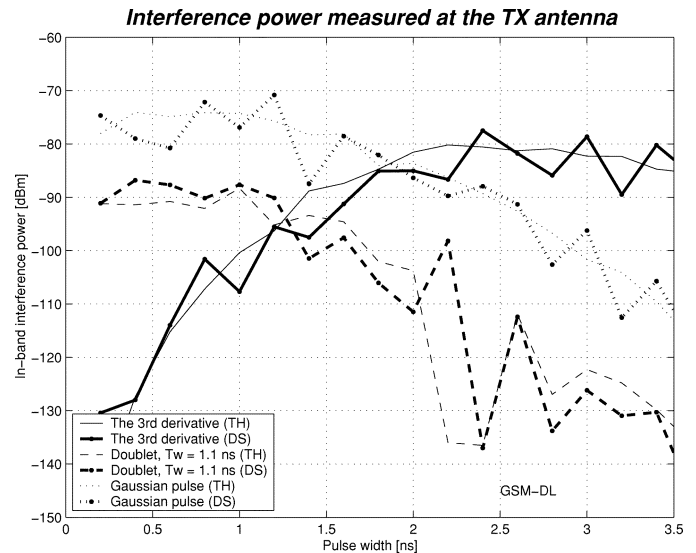


Fig. 6. In-band interference power as a function of the pulsewidth at GSM900 DL band.

spectrum overlaps the GSM band and the interference level reaches a maximum value. When the UWB pulsewidth is increased, the spectrum moves toward lower frequencies. If the pulsewidth is long (narrow) enough, the spectrum is below (above) the victim system's frequency band and interference does not occur.

As it can be seen from Figs. 5 and 6, the shorter pulsewidths favor the waveforms having the higher "center frequency." The limit at which the pulse waveform should be changed from the third derivative of the Gaussian pulse to the basic Gaussian pulse is about 2 ns, if the UWB pulse is selected from the GSM interference point-of-view. The Gaussian doublet in the figures generates a spectral null at about 909 MHz and, thus interfering less at the GSM UL band than the corresponding DL band. Changing the time gap between the consecutive pulses within the doublet affects even the interference level.

The difference between TH-UWB and DS-UWB is not significant. In the TH-UWB simulations, a  $T_f = 50$  ns is used. Also, the difference between UL and DL bands is insignificant from the in-band interference point of view.

#### B. UWB Interference at the UMTS/WCDMA Bands

UMTS/WCDMA systems utilize two different duplexing concepts: frequency-division duplex (FDD) and time-division duplex (TDD). In the beginning of the UMTS commercialization, only FDD will be used [8]. UMTS FDD UL and DL bands are between 1.92...1.98 GHz and 2.11...2.17 GHz, respectively. There will be two separate TDD bands between 1.9...1.92 GHz and 2.01...2.025 GHz [8]. Next, the in-band interference power levels are calculated using the UMTS channel bandwidth  $B = 3.84$  MHz.

Fig. 7 shows the interference power level in three UMTS bands when the UWB system is utilizing a generic Gaussian pulse. Both the TH-UWB and DS-UWB interference in UMTS/WCDMA bands are studied also in [9]. The results show that, from the UMTS band point of view, there are no significant differences in the interference between TH and DS concepts with Gaussian pulses.

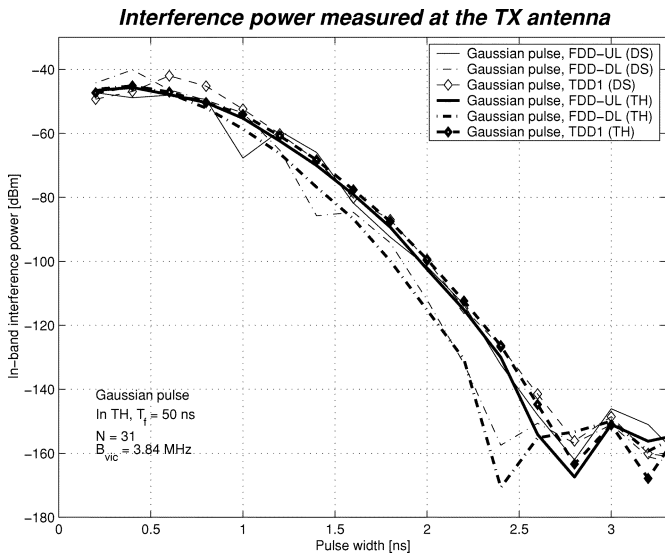


Fig. 7. In-band interference power caused by Gaussian pulse as a function of pulsewidth in UMTS bands.

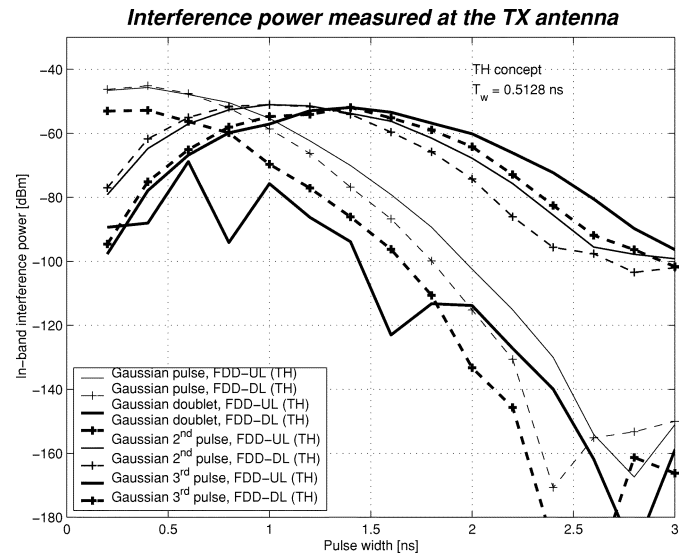


Fig. 9. In-band interference power in FDD-UL and FDD-DL bands caused by four different pulse waveforms. UWB system is based on TH concept.

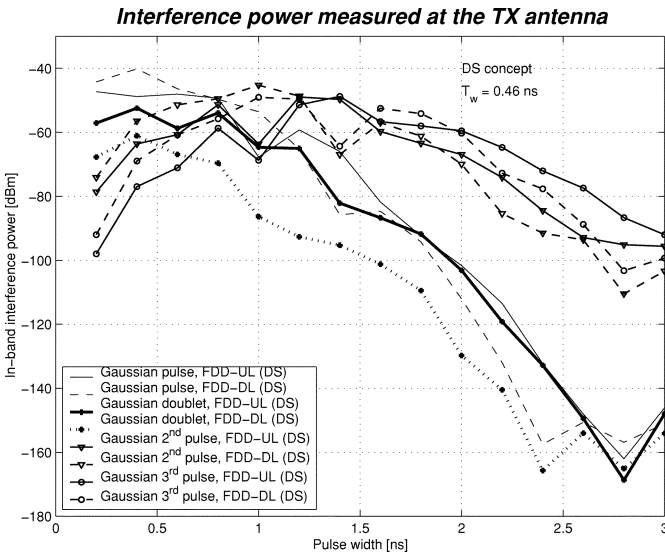


Fig. 8. In-band interference power caused by four different pulse waveforms using a DS-UWB system in FDD-UL and FDD-DL bands.

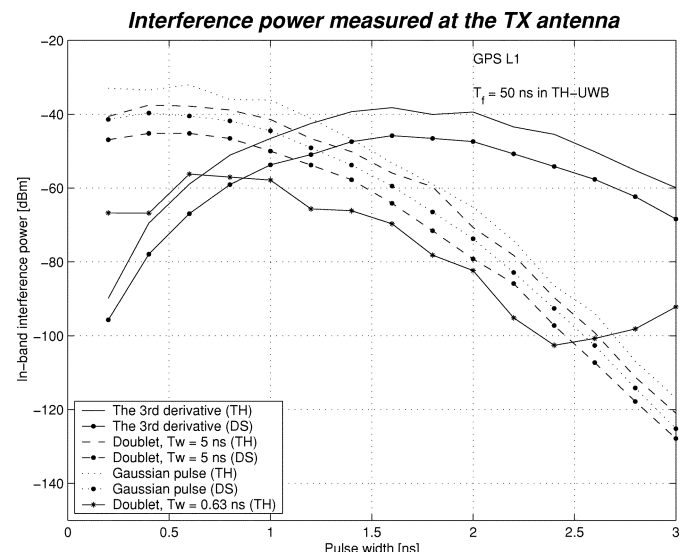


Fig. 10. In-band interference in GPS L1-band as a function of pulsewidth with three different pulse waveforms.

Fig. 8 shows the in-band interference power at UMTS FDD bands when the UWB system is based on DS, and four different pulse waveforms are used. The corresponding results for TH-UWB can be found in Fig. 9.

The effect of the different pulse repetition intervals are also studied at the UMTS/WCDMA frequency bands. Despite the different line spectra caused by the different  $T_f$ , the total in-band interference power seemed to be the same in all simulated cases, as the corresponding results from Fig. 7 show.

### C. UWB Interference at the GPS Bands

In the GPS system case, the L1-band and L2-band were selected for the detailed study. L1-band is used to carry the navigation information signal and the ionospheric delay is measured using L2-band [10]. In the calculations, a precise code P(Y) at 1.575 GHz (L1) and 1.227 GHz (L2) has been assumed. The information bandwidth (main lobe) for both channels is 20 MHz,

due to the 10 MHz maximum length code used in GPS system as the spreading code.

Fig. 10 shows the difference between TH and DS concepts when the interference power is calculated over the GPS L1-band [7]. The number of pulses used to transmit one data bit is the same in all the studied cases. The TH frame length is  $T_f = 50$  ns. The pulse separation  $T_w = 0.63$  ns in a doublet generates a spectral null at the L1-band. The effect can be seen as a smaller interference compared with the case where  $T_w = 5$  ns. The null separation in the latter case is 200 MHz, and there is no null at L1-band. In all cases studied, the DS concept causes less in-band interference power than the TH concept having the same system assumptions.

The corresponding results for GPS L2-band are presented in Fig. 11. The figure presents the results for both TH and DS systems. The results from Fig. 11 correspond to the results from Fig. 10, but the maximum interference appears at the different

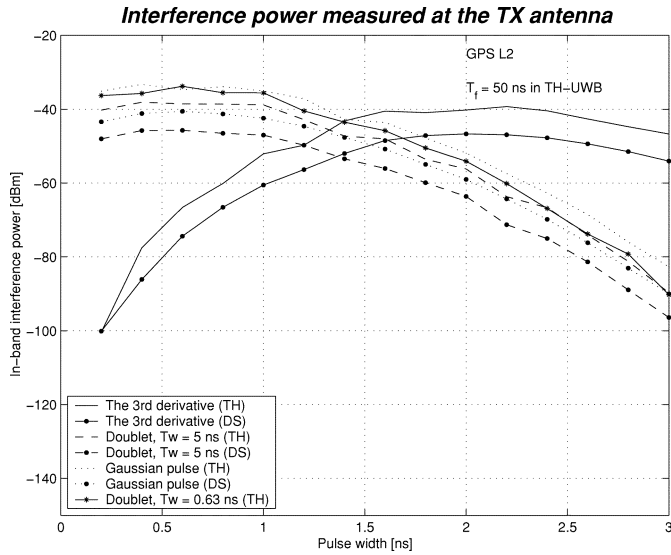


Fig. 11. In-band interference in GPS L2-band as a function of pulsewidth with three different pulse waveforms.

pulsewidths, due to the difference between L1 and L2 frequency bands.

To achieve high data rates and accurate positioning capability in IR systems, the pulsewidths should be  $\sim 1$  ns, or less. Keeping this in mind, the third derivative of the Gaussian pulse among the waveforms included in the study seems to be best choice from the interference point of view. This is valid for both L1- and L2-bands.

#### IV. NARROWBAND INTERFERENCE AGAINST UWB

In this section, we present a reverse coexistence study, with respect to the previous study, i.e., the interference is now coming from different narrowband systems (compared with the UWB system bandwidth) and its effect is shown by the study of the UWB system performance degradation.

The generated UWB pulse waveforms in the study are the Gaussian pulse and the second derivative of the Gaussian pulse. The pulse waveform in the channel is again the differentiation of the generated pulse. The processing gain of the UWB system has been fixed to  $PG = 20$  dB. The processing gain of TH-UWB is a combination of the pulse repetition coding and the low duty cycle. In DS-UWB, it is defined by the spreading factor (pulse repetition coding) only, as it can be noted in the following:

$$PG_{TH} = 10 \log_{10}(N) + 10 \log_{10} \left( \frac{T_f}{T_p} \right) \quad (9a)$$

and

$$PG_{DS} = 10 \log_{10}(N). \quad (9b)$$

The received UWB signal  $r(t)$  for the  $m$ th user can be modeled by

$$r^{(m)}(t) = s^{(m)}(t) + n(t) + J(t) \quad (10)$$

where  $n(t)$  and  $J(t)$  represents the noise and the interference, respectively. The transmitted signal  $s^{(m)}(t)$  is defined by (2) or

(3). At the receiver the signal is detected by a correlator, whose template waveform corresponds to the transmitted signal waveform. Correlation results are integrated over  $N$  pulses in order to form the data bit. When the antennas are modeled as derivators (high-pass filters) the received waveforms after the RX-antenna are the second derivatives of the generated waveforms.

The UWB system performance degradation in the presence of interference has been studied as a function of the SNR for several pulsewidths using a fixed total interference power level. Both TH and DS concepts have been implemented and the data modulation in UWB systems is BPAM, as in the earlier cases. No diversity methods at the reception are used. Perfect synchronization between the transmitter and the receiver is also assumed.

The simulation results are bit error rate (BER) curves as functions of both the desired UWB transmission SNR and of the total interfering power. The reference curve in the following figures is the theoretical upper bound limit for BPAM modulated signal in AWGN channel, which is also the upper bound performance limit for BPSK. The theoretical upper bound limit  $P_e$  can be calculated using [11]

$$P_e = Q \left( \sqrt{2 \frac{E_b}{N_0}} \right) \quad (11)$$

where  $E_b$  is the bit energy, and  $N_0$  the noise power spectral density.

##### A. Multitone Jamming at the GSM Band

First, the UWB system performance degradation is studied in the presence of multitone jamming at GSM900 bands [12]. In an AWGN channel, the multitone jamming is added to the propagating UWB signal. Both the GSM uplink and GSM downlink jamming cases were studied. The bandwidth of the GSM channel is only 200 kHz, a minor fraction of the UWB bandwidth. This allows us to model the GSM signal (physical channel) as a tone and without any modulation scheme to spread the spectrum. Ten independent interfering tones are used to describe the GSM signals. The physical channels 0 and 124 of the GSM system are always allocated, while the eight other channels are randomly selected inside the GSM band. This maximizes the jamming spectral allocation, while still offering reasonable simulation times. The GSM channel allocation for the eight tones is renewed each time the SNR is changed in the simulation. The random phases for each of the jamming tone signals are updated when the data bit is changed.

Fig. 12 shows the BERs for the first derivative of the Gaussian pulse used in the TH-UWB and the DS-UWB systems. The legends in the figures define the corresponding radiated UWB signal waveform and system concept. Performance curves are presented for several pulsewidths suitable for high data rate UWB communication applications. The power of the UWB signal under interest is set to 0 dBm. The observed total interference power at the GSM bands at the receiver antenna is 15 dBm, in all cases. The jamming signal power is evenly distributed over the ten tones. This assumption yields a total signal-to-jamming ratio ( $S/J$ ) of  $-15$  dB. Corresponding results for the Gaussian third derivative as a radiated waveform are shown in Fig. 13.

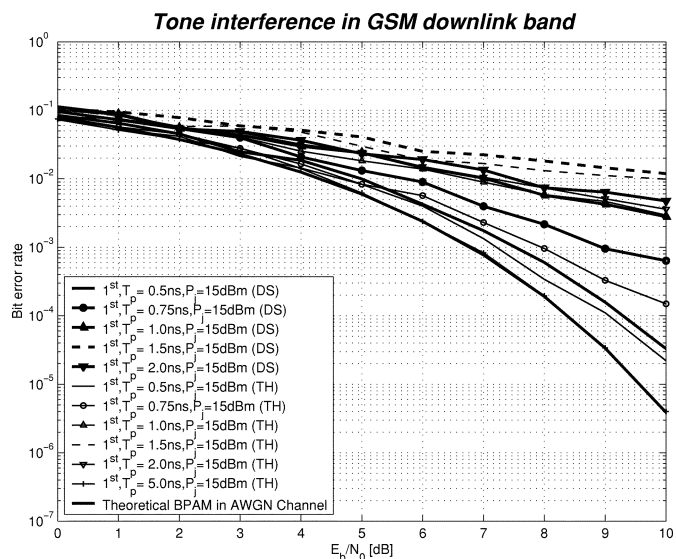


Fig. 12. BERs for TH-UWB and DS-UWB systems. The radiated waveform is the first derivative of the Gaussian pulse. Multitone interference is in GSM DL-band, and total interference power is 15 dBm.

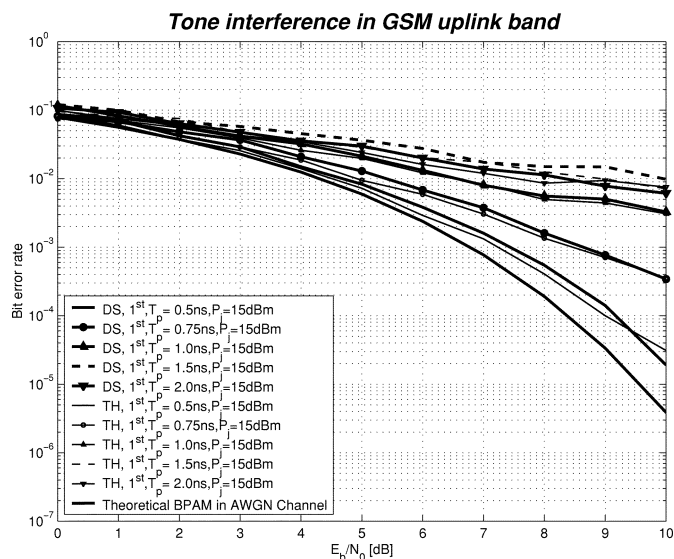


Fig. 14. BERs for TH-UWB and DS-UWB systems. The radiated waveform is the first derivative of the Gaussian pulse. Multitone interference is in GSM UL-band, and total interference power is 15 dBm.

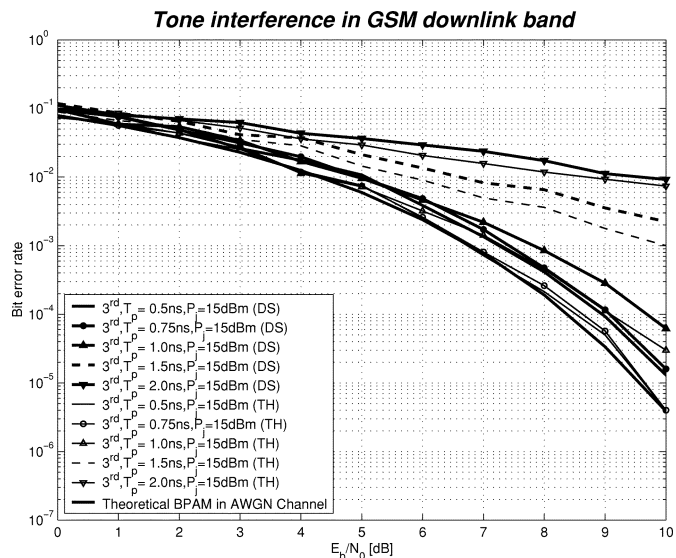


Fig. 13. BERs for TH-UWB and DS-UWB systems. The radiated waveform is the third derivative of the Gaussian pulse. Multitone interference is in GSM DL-band, and total interference power is 15 dBm.

The results show that the performance of the TH-UWB system is slightly better than the referred DS-UWB one. Our results express that the SNR difference between the concepts is about 0.5 dB ... 1 dB to achieve the same performance. Comparing Figs. 12 and 13 to see the effect of the pulse waveform, one can notice that the Gaussian third derivative leads to better performances than the Gaussian first derivative when  $T_p < 2$  ns. This is valid for both TH- and DS-concepts.

In Fig. 14, the corresponding results for the Gaussian first derivative are calculated for the GSM UL band. Since the channel allocation between GSM uplink and downlink channels is small, the results correspond almost to the ones shown in Fig. 12. However, some individual differences related to the different spectral allocation can be noticed.

If we compare the UWB signal spectra from Fig. 2, one can notice that the signal level of the Gaussian pulse is about 15 dB

higher than the signal of the second derivative of the Gaussian pulse in the GSM DL band. This suggests that the latter system tolerates 15 dB higher interference power, still achieving the same system performance. Generalizing this comparison, we conclude that the results discussed here can be applied to a broad range of interference levels by calculating the jamming margin directly from the spectrum of the pulse.

In general, the UWB system performance degrades when the pulsewidth increases. This roots from the spectral shape of the UWB signal. Gaussian first derivative with  $T_p = 1$  ns yields the center frequency at 1 GHz, which is close to the interference source. Respectively, Gaussian third derivative with  $T_p = 2$  ns yields  $f_c = 865$  MHz. Being a relatively narrowband interference around the vicinity of 950 MHz, the GSM downlink carrier resembles a pulse whose width is matched close to the UWB signal. By setting  $T_p$  small enough, the UWB spectrum moves to the higher frequencies and eventually out of the range of the interfering frequency. This explains the improvement in the performances of the UWB system using narrow pulses. In the absence of jamming, all the curves in Figs. 12–14 would fall on the theoretical performance curve. Changing the center frequency of the narrowband interference, the performance results would be different.

Decreasing  $T_p$  or increasing the order of the derivative of the radiated waveform, the power spectral density will be shifted toward higher frequencies, giving a larger jamming margin against GSM interference in both the TH-UWB and the DS-UWB systems.

### B. Pulsed Jamming Interference at the UMTS FDD Bands

In this section, we discuss the UWB system performance under pulsed jamming interference at the UMTS/WCDMA bands in an AWGN channel. In this case, the UMTS frequency band is assumed to be fully loaded. This means that in the FDD band, the total interfering UMTS signal power is evenly spread over the 60-MHz band. Thus, the UMTS signals are modeled using a sinc wave having a rectangular spectrum with

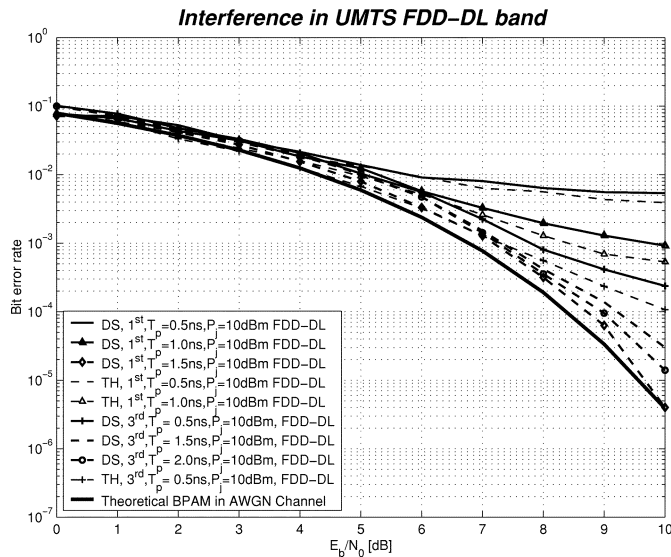


Fig. 15. BERs for UWB systems in presence of interference in the UMTS FDD DL band.

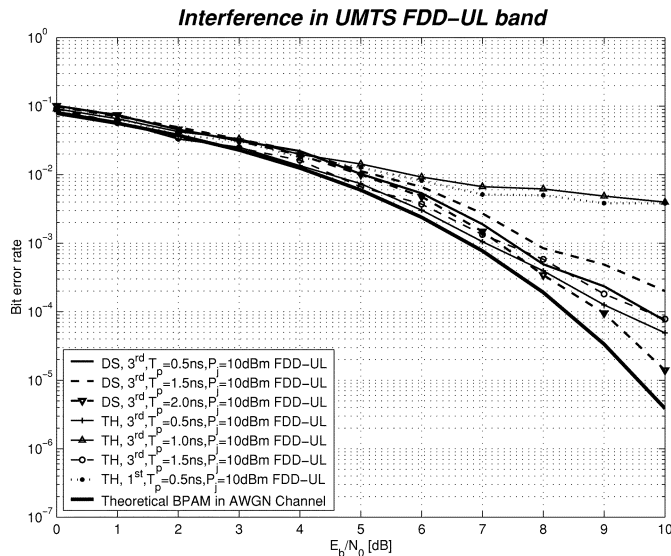


Fig. 16. BERs for UWB systems in presence of interference in the UMTS FDD UL band.

a 60-MHz bandwidth. As a matter of fact, even a single UMTS signal can be considered a narrowband signal in our study, since its bandwidth is much smaller than the one related to any UWB signal.

In Fig. 15, the interference has been studied in the UMTS FDD DL band. Corresponding results for the UL band can be seen in Fig. 16. In both cases, the first and the third derivatives of the Gaussian pulse (generated pulse waveforms) have been considered in the performance analysis. The observed total interference power is 10 dBm in all cases.

The results from Fig. 15 show that TH-UWB performs slightly better than DS-UWB, just as in GSM. This can be easily noticed when the interference starts to be negligible; TH-UWB performances are going to superimpose the theoretical curve, while DS-UWB ones remain slightly higher. The difference between the two systems is about 1 dB. A

particular situation can be noticed using the first derivative of the Gaussian pulse, where the two systems perform in a similar fashion. Furthermore, by using longer pulses, the theoretical performance in AWGN channel can be reached. This is due to the fact that the UWB spectrum related to those longer pulses is shifted below the interfering frequencies. The BER degradation can be considered a linear function of the increasing interfering signal power.

According to the results, the performance is worst when the center frequency  $f_c$  of the UWB pulse (shown in Table I) overlaps the interfering signal band. This is valid for both the TH-UWB and DS-UWB systems.

The results also indicate that when longer pulses are transmitted, UWB system performance is better in the presence of UMTS/WCDMA interference if the first derivative of a Gaussian pulse is used rather than the third. High data rate applications demand short pulses; thus, the third derivative of the Gaussian pulse performs best, amongst the simulated waveforms. The same was noticed also in the GSM case. The difference in performance comes from the different spectral allocations, compared with the interfering UMTS signals. Considering the pulse waveforms in the channel, the center frequency of the third derivative of the Gaussian pulse is 1.73 times higher than the corresponding  $f_c$  of the first one.

## V. CONCLUSION

In this paper, in-band interference and jamming power, caused by several pulse waveforms generating UWB spectrum, have been studied. Also, performance degradation of an UWB system in an AWGN channel, in the presence of narrowband interference is presented. In the in-band interference study, the victim radio systems are UMTS/WCDMA, GSM900, and GPS. UWB systems under consideration are based on baseband binary-PAM modulation, utilizing both the TH and the DS concepts.

The results show that proper selection of UWB pulse waveform and width pave the way for spectral planning. UWB interference noticed by other RF systems depends on those selections. Using short pulses, interference in the frequency bands studied is the smallest if the pulse waveform is based on higher order Gaussian waveforms. On the other hand, long pulses favor the generic Gaussian pulse. According to the results, DS based UWB systems seem to interfere less than the corresponding TH systems in the GPS channel. The difference between TH-UWB and DS-UWB was insignificant on the other simulated frequency bands. Due to the assumptions of the study, the UWB data rates are different in the corresponding cases.

When the UWB system degradation is studied in the presence of an interfering and jamming radio system, results show that the system performance suffers most if the interference and the nominal center frequency of the UWB system are overlapping. Thus, the UWB performance depends on the pulse waveform and on the pulsewidth. When there is a demand for high data rates, short pulses should be used. Thus, in this case, the third derivative of the Gaussian pulse performs better than the first derivative. On the other hand, if the data rate demands are not so high, and long pulses can be used, lower order waveforms

perform better. The degradation of the system performances is also a linear function of the increasing interference power.

Our future work will include different UWB system performances with multiband interference using real channel model [13] instead of AWGN channel. Also, other data modulation schemes than BPAM will be taken into account.

#### ACKNOWLEDGMENT

The authors would like to thank student N. Laine [M.Sc. (Tech.)] for her assistance during the computer simulations and G. Lehtola [M.Sc. (Mat.)] for the language checking.

#### REFERENCES

- [1] "First Report and Order in the Matter of Revision of Part 15 of the Commission's Rules Regarding Ultra-Wideband Transmission Systems," FCC, released, ET Docket 98-153, FCC 02-48, Apr. 22, 2002.
- [2] R. A. Scholtz and M. Z. Win, "Impulse radio," in *Wireless Commun., TDMA Versus CDMA*, S. Glicic and P. Leppänen, Eds. London, U.K.: Kluwer, 1997, pp. 245-263.
- [3] R. Fleming and C. Kushner, "Warfighter visualization PI meeting," presented at the Ultra-Wideband Localizers, Oct. 18, 2000.
- [4] F. Ramirez-Mireles and R. A. Scholtz, "System performance analysis of impulse radio modulation," presented at the Radio and Wireless Conf., Colorado Springs, CO, 1998.
- [5] H. F. Harmuth, *Antennas and Waveguides for Nonsinusoidal Waves*. New York: Academic, 1984.
- [6] M. Mouly and M. Pautet, *The GSM System for Mobile Communications*. Palaiseau, France: Telecom, 1992.
- [7] M. Hämäläinen, J. Iinatti, V. Hovinen, and M. Latva-aho, "In-band interference power of three kind of UWB signals in GPS, L1-band and GSM900 bands," in *Proc. IEEE PIMRC Conf.*, 2001, pp. D76-80.
- [8] H. Holma and A. Toskala, Eds., *WCDMA For UMTS: Radio Access Third-Generation Mobile Communications*. New York: Wiley, 2000.
- [9] M. Hämäläinen, V. Hovinen, J. Iinatti, and M. Latva-aho, "In-band interference power caused by different kinds of UWB signals at UMTS/WCDMA frequency bands," in *Proc. RAWCON2001 Conf.*, 2001, pp. 97-100.
- [10] [Online]. Available: [http://www.colorado.edu/geography/gcraft/notes/gps/gps\\_f.html](http://www.colorado.edu/geography/gcraft/notes/gps/gps_f.html).
- [11] L. W. Couch, II, *Digital and Analog Communication Systems*. New York: Macmillan, 1983.
- [12] M. Hämäläinen, V. Hovinen, and J. Iinatti, "Performance comparison between various UWB signals in AWGN channel in the presence of multitone interference at the GSM downlink band," in *Proc. WPMC Conf.*, 2001, pp. 449-453.
- [13] V. Hovinen, M. Hämäläinen, and T. Pätsi, "Ultra wideband indoor radio channel models: Preliminary results," in *Proc. IEEE Conf. Ultra-Wideband Syst. Techni.*, 2002, pp. 75-79.



**Matti Hämäläinen** (S'94) was born in Sodankylä, Finland, in 1967. He received the M.Sc. degree in electrical engineering and the Lic. Tech. degree from the University of Oulu, Oulu, Finland, in 1994 and 2002, respectively, where he is working toward the Ph.D. degree.

He has been with Telecommunication Laboratory, University of Oulu, since 1993. Since 1999, he has been with the Centre for Wireless Communications, Telecommunication Laboratory, University of Oulu, as a Researcher and a Project Manager. His research interests are wideband radio channel modeling, spread spectrum communications, and UWB systems.

Mr. Hämäläinen is a Member of the IEEE Communication and Antennas and Propagation Societies.



**Veikko Hovinen** (S'02) received the M.Sc. degree in electrical engineering from the University of Oulu, Oulu, Finland, in 1993.

Since 1990, he has been working with the Telecommunications Laboratory, University of Oulu. In 1998, he joined the UWB team at the Centre for Wireless Communications (CWC), University of Oulu. His interests are UWB radio systems and channel modeling.



UWB radio systems.

**Raffaello Tesi** (S'98) was born in Pistoia, Italy, in 1976. In 2001, he received the "Laurea" (M.Sc.) degree in telecommunications engineering from the University of Florence, Florence, Italy, with a thesis on transmit diversity in Satellite-UMTS. He is currently working toward the Ph.D. degree from the University of Oulu, Oulu, Finland

In 2000, he joined the Centre for Wireless Communications (CWC), University of Oulu, where he is currently a Research Scientist. His main fields of interest include satellite mobile communications and



he has been working as a Professor at the University of Oulu and as a Senior Research Scientist, Project Manager, and Research Director at the Centre for Wireless Communications (CWC), University of Oulu. His research interests are in future wireless communication systems and algorithms.

Dr. Iinatti is a Member of the IEEE Communication, IEEE Signal Processing, and IEEE Information Theory Societies.

**Jari H. J. Iinatti** (M'95) was born in Oulu, Finland, in 1964. He received the M.Sc. degree in electrical engineering, and the Lic. Tech. and Dr. Tech. degrees, in 1989, 1993, and 1997, respectively, all from the Department of Electrical Engineering, University of Oulu, Oulu, Finland.

Since 1989, he has been a Research Scientist at the Telecommunication Laboratory, University of Oulu, where he belongs to the spread-spectrum research group. He finished his Doctoral Thesis, dealing with code acquisition, in 1997. Since 1997,



**Matti Latva-aho** (S'96-M'98) received the M.Sc. degree in electrical engineering, and the Lic. Tech. and Dr. Tech. degrees from the University of Oulu, Oulu, Finland, in 1992, 1996, and 1998, respectively.

From 1992 to 1993, he was a Research Engineer at Nokia Mobile Phones, Oulu. From 1994 to 1998, he was a Research Scientist at the Telecommunication Laboratory and Centre for Wireless Communications (CWC), University of Oulu. Currently, he is the Director of the CWC, and Professor of Digital Transmission Techniques at the Telecommunications Laboratory. His research interests include future broadband wireless communication systems and related transceiver algorithms. He has published more than 50 conference or journal papers in the field of CDMA communications.

Dr. Latva-aho is serving as the Chairman of the IEEE Communications Society Finland Chapter from 2002 to 2003.